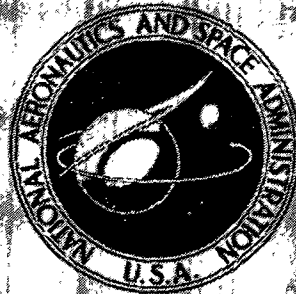


NASA TECHNICAL  
MEMORANDUM



N73-11012  
NASA TM X-2638

NASA TM X-2638

# CASE FILE COPY

## SMALL-SCALE TESTS OF THE MIXER NOZZLE CONCEPT FOR REDUCING BLOWN-FLAP NOISE

*by Jack H. Goodykoontz, William A. Olsen,  
and Robert G. Dorsch*

*Lewis Research Center*

*Cleveland, Ohio 44135*

NATIONAL AERONAUTICS AND SPACE ADMINISTRATION • WASHINGTON, D. C. • NOVEMBER 1972

1. Report No. NASA TM X-2638		2. Government Accession No.		3. Recipient's Catalog No.	
4. Title and Subtitle SMALL-SCALE TESTS OF THE MIXER NOZZLE CONCEPT FOR REDUCING BLOWN-FLAP NOISE				5. Report Date November 1972	
				6. Performing Organization Code	
7. Author(s) Jack H. Goodykoontz, William A. Olsen, and Robert G. Dorsch				8. Performing Organization Report No. E-6999	
9. Performing Organization Name and Address Lewis Research Center National Aeronautics and Space Administration Cleveland, Ohio 44135				10. Work Unit No. 741-89	
				11. Contract or Grant No.	
12. Sponsoring Agency Name and Address National Aeronautics and Space Administration Washington, D. C. 20546				13. Type of Report and Period Covered Technical Memorandum	
				14. Sponsoring Agency Code	
15. Supplementary Notes					
16. Abstract Noise tests were conducted using simulated mixer-type nozzles and a small-scale model of an externally-blown-flap lift-augmentation system. The mixer nozzles were simulated with orifice plates. The wing model had a chord length of 32.4 cm and a span of 61 cm. The wing had two flaps that could be placed in three different settings: (1) leading flap 30° from the wing chord line, trailing flap 60° from the chord line; (2) leading flap 10° from the chord line, trailing flap 20°; and (3) both flaps at a 0° angle with respect to the wing chord line (i.e., retracted). Noise data were taken for two different-size mixer orifices. The first orifice plate consisted of eight round-ended trapezoidal-shaped openings with an equivalent diameter of 6.0 cm (total open area equal to that of a single 6.0-cm-diam orifice). The results showed that when used with the 30°-60° flaps, this orifice plate was 6 dB quieter, under the wing, than a single circular orifice with the same area. With the 10°-20° flap setting, the eight-lobe mixer orifice was approximately 2 dB quieter than the single orifice. Results are also presented for variations to the eight-lobe mixer orifice - wing - flap system. The second mixer orifice consisted of sixteen 1.03-cm-diameter holes arranged in a square pattern. The equivalent diameter was 4.1 cm. With the 30°-60° flaps, this orifice was from 4 to 5 dB quieter than a single circular orifice with the same area.					
17. Key Words (Suggested by Author(s)) Acoustics; Aerodynamic noise; Aircraft noise; Jet aircraft noise; Lift augmentation; Noise (sound); Nozzles; Short takeoff aircraft; Wing flaps			18. Distribution Statement Unclassified - unlimited		
19. Security Classif. (of this report) Unclassified		20. Security Classif. (of this page) Unclassified		21. No. of Pages 33	22. Price* \$3.00

# SMALL-SCALE TESTS OF THE MIXER NOZZLE CONCEPT FOR REDUCING BLOWN-FLAP NOISE

by Jack H. Goodykoontz, William A. Olsen, and Robert G. Dorsch  
Lewis Research Center

## SUMMARY

Noise tests were conducted using simulated mixer-type nozzles and a small-scale model of an externally-blown-flap lift-augmentation system. The mixer nozzles were simulated with orifice plates. The wing model had a chord length of 32.4 centimeters and a span of 61 centimeters. The wing had two flaps that could be placed in three different settings: (1) leading flap  $30^{\circ}$  from the wing chord line, trailing flap  $60^{\circ}$  from the chord line; (2) leading flap  $10^{\circ}$  from the chord line, trailing flap  $20^{\circ}$ ; and (3) both flaps at a  $0^{\circ}$  angle with respect to the wing chord line (i.e., retracted).

Noise data were taken for two different-size mixer orifices. The first orifice plate consisted of eight round-ended trapezoidal-shaped openings with an equivalent diameter of 6.0 centimeters (total open area equal to that of a single 6.0-cm-diam orifice). The results showed that when used with the  $30^{\circ}$ - $60^{\circ}$  flaps, this orifice plate was 6 decibels quieter, under the wing, than a single circular orifice with the same area. With the  $10^{\circ}$ - $20^{\circ}$  flap setting, the eight-lobe mixer orifice was approximately 2 decibels quieter than the single orifice. Results are also presented for variations to the eight-lobe mixer orifice - wing - flap system.

The second mixer orifice consisted of sixteen 1.03-centimeter-diameter holes arranged in a square pattern. The equivalent diameter was 4.1 centimeters. With the  $30^{\circ}$ - $60^{\circ}$  flaps, this orifice was from 4 to 5 decibels quieter than a single circular orifice with the same area.

## INTRODUCTION

One method to increase the lift capability of a STOL aircraft during takeoff and landing is to incorporate an externally-blown-flap system. With this method, large trailing-edge wing flaps are lowered directly into the fan-jet engine exhaust. Unfortunately, the

impingement of this high-velocity airstream on the flap surfaces causes a substantial increase in the noise level of the engine exhaust jet. In order to meet the frequently suggested goal for STOL aircraft of 95 effective perceived noise decibels (EPNdB) at the 500-foot sideline, the additional noise generated by the interaction of the jet exhaust with the flaps must be considerably reduced.

The flap interaction noise appears to be proportional to the surface area of the flaps scrubbed by the jet exhaust and to the sixth power of the jet exhaust impingement velocity. Reducing this impingement velocity (while maintaining acceptable lift characteristics) appears to offer promise of substantial reduction in flap interaction noise.

The impingement velocity can be reduced by employing a mixer nozzle at the fan-jet engine exhaust. A mixer nozzle is a multielement nozzle designed in such a way that the velocity of the individual small jets making up the exhaust decays rapidly by turbulent mixing with the surrounding low-velocity airstream.

This report presents experimental results on the noise reduction effectiveness of a mixer nozzle. Noise measurements were made with a small-scale (32.4-cm wing chord) externally-blown-flap model using the mixer nozzle concept to reduce the velocity of impingement at the flaps. Orifice plates were used, instead of nozzles, to simplify the apparatus.

Two sets of mixer-type nozzle data are presented. The first set of data presents the results obtained from a single orifice and an eight-lobe, round-end trapezoidal orifice, both having an equivalent diameter of 6.0 centimeters. The eight-lobe orifice was used since, in reference 1, it was found that this configuration gave a high rate of axial velocity decay. The second set of data presents the results obtained from a single orifice and a multihole orifice having equivalent diameters of 4.1 centimeters. The effectiveness of the mixer-type (multielement) orifices was assessed by comparing the noise data obtained with the mixer orifices with data from the same-equivalent-diameter single orifice.

In addition, data are presented for variations to the orifice-wing-flap system (using the eight-lobe orifice). These data were taken in an effort to reduce and/or isolate the noise generated by the high-velocity jet scrubbing action.

## SYMBOLS

C nozzle (orifice) discharge coefficient

$D_e$  equivalent diameter,  $\sqrt{\frac{4 \times \text{total area}}{\pi}}$ , cm

$M_j$  Mach number at nozzle (orifice) exit

$V$  free-stream peak jet velocity, m/sec  
 $V_j$  peak velocity at nozzle (orifice) exit plane, m/sec  
 $x$  axial distance from nozzle (orifice) exit plane, cm

## APPARATUS AND PROCEDURE

Two facilities were used to obtain the experimental data presented herein. Basically, they were identical in mechanical and electronic hardware and mode of operation. However, the distance from the ground surface to the centerline of the orifices was different for the two facilities. This distance was 1.22 meters for the first facility and 1.52 meters for the second facility. In addition, the two facilities were located at different sites on the laboratory property. The majority of the data was taken at the first site. The second site was used primarily to obtain the data for the variations to the model (e.g., slots covered). Comparison of the data obtained at the two sites for the same configuration showed an overall-sound-pressure-level (OASPL) repeatability of within 2 decibels and a sound-pressure-level (SPL) repeatability of within 2 decibels in the middle frequency range and within 4 decibels at the high end of the frequency range. The following descriptions of the apparatus and procedure apply to both facilities.

### Flow System

The data were obtained by using the experimental apparatus shown in figures 1 and 2. The flow system (fig. 1) consisted of an orifice for flow measurement, a 10.16-centimeter flow control valve, a muffler section, a long straight section of 10.22-centimeter-diameter pipe, and the test orifices. Cold air (294 K) flowed through the test orifices and impinged on the wing-flap system.

The muffler section was installed to reduce the noise generated by the globe-type flow control valve. It consisted of a series of perforated plates and a tuned dissipative muffler. A more thorough discussion of the muffler section is presented in reference 2.

### Externally-Blown-Flap Model

Wing-flap assembly. - The model that was tested in this experiment is shown in figure 2. The wing and flaps (fig. 2(a)) were made of wood covered with fiberglass and were smoothed and polished. The wing had a chord length of 32.4 centimeters with the flaps retracted and a span of 61 centimeters. The flaps could be placed in the  $30^{\circ}$ - $60^{\circ}$

position (with respect to the wing chord line), the  $10^{\circ}$ - $20^{\circ}$  position, and the  $0^{\circ}$  (retracted) position. The distance from the orifice centerline to the underside of the wing was 7.62 centimeters measured at the orifice exit. The wing was oriented to give a  $5^{\circ}$  angle of attack between the wing chord line and the centerline of the orifice. The distance from the orifice exit to the  $60^{\circ}$  flap, measured along the orifice centerline, was 29.55 centimeters for one pair of orifices ( $D_e = 6.0$  cm) and 37.0 centimeters for the other pair of orifices ( $D_e = 4.1$  cm).

A variation to the wing-flap system, with the flaps in the  $10^{\circ}$ - $20^{\circ}$  setting, consisted of blocking off the slots between the fixed wing and leading flap and between the two flaps. This was done with a thin-gage metal shield that covered the entire bottom side of the wing-flap system. Also, a partial-span shield 12.7 centimeters wide that covered both slots and was centered about the centerline of the orifice was used in some tests. The eight-lobe orifice ( $D_e = 6.0$  cm) was used with these configurations.

An additional variation to the wing-flap system, again with the flaps in the  $10^{\circ}$ - $20^{\circ}$  position, included alternate blocking of the slots. First, the front slot between the fixed wing and the leading flap was covered with a thin metal plate that extended the entire span of the model. The rear slot between the flaps remained open. The arrangement was then reversed with the rear slot covered and the front slot open. Again, the eight-lobe orifice was used for this test.

Figure 2(b) shows the facility with the wing flaps in the  $30^{\circ}$ - $60^{\circ}$  position and the eight-lobe orifice installed.

Test orifices. - Data were obtained from two different pairs of orifice plates. Each pair included an orifice plate with a single circular opening and an orifice plate with multielement openings. The total open areas for the two configurations of a given pair were the same; consequently, the equivalent diameters were the same. In addition, the discharge coefficients for a given pair were approximately the same.

Figure 2(c) shows the dimensions and configuration of the orifices with an equivalent diameter of 6.0 centimeters (nominal). Discharge coefficients of the orifices (ratio of actual airflow rate to ideal airflow rate) in figure 2(c) were approximately 0.8. The exit area of the single-hole orifice is the same as the total exit area of the eight-lobe orifice.

A variation to the eight-lobe orifice consisted of placing a fine-mesh wire screen over the three openings nearest the wing. This was done to reduce the jet velocity near the wing in an effort to lower the sound generated by the scrubbing action of the jet on the wing.

Figure 2(d) shows the dimensions and configuration of the orifices with an equivalent diameter of 4.1 centimeters (nominal). The multihole orifice plate had sixteen 1.03-centimeter-diameter holes arranged in a square pattern as shown. The multihole orifice plate was mounted in the facility so that a side of the square array was parallel to the

underside of the wing. The discharge coefficient for the multihole orifice was 0.67, and the coefficient for the single orifice was 0.61.

## Instrumentation

The noise data were measured by fourteen 1.27-centimeter-diameter condenser microphones placed at various intervals on a 3.05-meter-radius circle centered at the orifice exit. The microphone horizontal plane and jet centerline were located 1.22 and 1.52 meters, respectively, above a smooth flat asphalt surface. Windscreens were placed on all microphones.

Total pressure upstream of the test orifices and static pressure upstream of the flow metering orifice were measured with precision Bourdon tube pressure gages. The pressure drop across the flow metering orifice was measured with a U-tube manometer filled with glycol. Temperatures were measured upstream of the test orifices and the flow metering orifice with immersion-type thermometers.

Weather data (barometric pressure, humidity, and wind speed and direction) were also monitored and/or recorded.

## Procedure

Free-stream velocities with the wing removed were calculated from total pressures measured downstream of the orifices by a traversing probe. The static pressure in the free stream was assumed to be atmospheric. The total temperature at the probe was assumed to be the same as the temperature measured upstream of the orifices.

Far-field noise data and flow data were taken for various pressure ratios across the test orifices. The test procedure was to obtain a steady flow condition for a given total pressure upstream of the test orifice. The majority of the data were taken with the spanwise direction of the wing in the vertical position and the plane of the microphone circle perpendicular to the wing. A limited amount of data were taken with the wing in the horizontal position so that sideline noise tests could be simulated.

Three noise data samples were taken at each of the 14 microphone locations. A total of 20 minutes were required for this sampling. The noise data were analyzed directly by a 1/3-octave-band spectrum analyzer which determined sound pressure level (SPL) spectrums referenced to  $2 \times 10^{-5}$  N/m<sup>2</sup>. An atmospheric loss correction was applied to the average of the three samples, and an overall sound pressure level (OASPL) was computed for each microphone position. Additional filters were used (1/3-octave center frequencies of 25, 31.5, and 40 kHz) for a limited number of runs to investigate the high-frequency characteristics of the SPL spectra.

The condenser microphones were calibrated before each run with a standard piston calibrator (124 dB±0.2 dB, 250-Hz tone). The 1/3-octave-band analyzer was calibrated before the test with a constant-voltage source and checked during the experiment with an electronic pink noise generator. Additional assurance of the reliability of the electronic system was made by flowing air through an auxiliary orifice, analyzing the emitted sound, and examining the data to see if the results obtained from the current run agreed with a previous run.

## RESULTS AND DISCUSSION

### Peak Velocity Degradation

Free-stream velocity profiles downstream of the orifices with an equivalent diameter of 6.0 centimeters are shown in figures 3 and 4.

Figure 3 shows the velocity profiles for the eight-lobe orifice at three axial positions. Near the exit (fig. 3(a)), the profile has a double peak since the flow field is influenced by each individual jet. At the location shown ( $x = 15.2$  cm) the peak jet velocity has been reduced to 75 percent of the orifice exit velocity.

At an axial distance of 29.6 centimeters (fig. 3(b)), the influence of each jet is less and the peak velocity has been reduced to about 64 percent of the orifice exit velocity. This axial distance ( $x = 29.6$  cm) is the same distance as that from the orifice exit to the 60° flap, measured along the orifice axis, when the wing is in place. As the axial distance increases further (fig. 3(c)), the individual peaks vanish and the flow coalesces into one large jet.

Figure 4 shows the velocity profile from the single orifice measured at an axial distance of 29.6 centimeters downstream from the orifice exit. The peak velocity is approximately the same as the orifice exit velocity (290 m/sec).

The velocity profiles at 37 centimeters downstream of the orifice exit for the 4.1-centimeter-equivalent-diameter orifices are shown in figure 5. This axial position is at the impingement point on the 60° flap (measured along the orifice axis) when the wing is in place. The peak velocity for the multihole orifice at this axial position is approximately one-half of the velocity at the orifice exit. The peak velocity for the single orifice is approximately 70 percent of the exit velocity.

The velocity degradation results are summarized in figure 6. The ordinate is the ratio of the local free-stream peak jet velocity  $V$ , as measured at various axial positions, to the peak velocity at the exit plane of the orifice  $V_j$ . The velocity ratio is plotted as a function of an axial distance parameter which includes the axial distance downstream of the orifice exit  $x$ , the equivalent diameter of the orifices  $D_e$ , the orifice

discharge coefficient  $C$ , and the Mach number of the jet at the orifice exit  $M_j$ . The solid curve is representative of the velocity decay data for single nozzles and single orifices from an extensive experimental program reported in reference 1. The single-orifice data of the work reported herein agree reasonably well with the data represented by the curve. In addition, the eight-lobe and multihole orifices show a faster rate of velocity decay than do the single orifices with the same equivalent diameters. Therefore, the multielement orifices satisfactorily simulated a mixer-type nozzle in that a rapid velocity decay is induced.

## Sound Measurements with 6.0-Centimeter-Equivalent-Diameter Orifices

Orifice alone. - The noise data for the eight-lobe orifice alone at two orifice pressure ratios (or exhaust velocities) are compared in figure 7. The overall sound pressure level (OASPL) directivity at a distance of 3.05 meters (fig. 7(a)) is plotted for only one-half of the microphone circle since the sound pattern is symmetrical about the orifice axis. A considerable difference in level exists between the two examples since the sound pressure level is proportional to the eighth power of the velocity. The sound pressure level (SPL) 1/3-octave spectra (fig. 7(b)) again show a large difference in the levels for the two pressure ratios. The peak at 16 kilohertz for a pressure ratio of 1.23 is attributed to scatter in the data.

A comparison of the noise data for the eight-lobe orifice alone and the single orifice alone is shown in figure 8. In figure 8(a) the OASPL at a distance of 3.05 meters is shown. The orifice pressure ratio was 1.74 for both orifices. The differences in OASPL between the single and eight-lobe orifices are small to about  $120^\circ$ , with the level from the single orifice being about 2 decibels greater. Between  $120^\circ$  and  $160^\circ$  the separation increases to a maximum of about 5 decibels at  $160^\circ$ .

The sound pressure level 1/3-octave spectra for the orifices alone are shown in figure 8(b). The single-orifice spectrum was measured at  $90^\circ$  from the engine inlet, and the eight-lobe-orifice spectrum was measured at  $80^\circ$ . Below a center frequency of 6300 hertz the single-orifice level is higher than the eight-lobe orifice level. In the high-frequency range the sound level of the eight-lobe orifice would be higher than that of the single orifice as a result of the smaller individual flow passages of the eight-lobe orifice.

Orifices with wing. - Comparison of the noise data for the eight-lobe orifice and the wing with various flap settings is shown in figure 9. Also shown are the data for the orifice alone. A pressure ratio of 1.74 was used for all runs. In figure 9(a), the OASPL with the wing in place is shown to be greater below and forward of the wing ( $0^\circ$  to  $160^\circ$ ) for a given flap setting. The noise produced with the wing in place is made up of interaction of the jet exhaust and the wing-flap system and reflection of the noise generated by the nozzle alone. As the flap angles decrease, the sound pressure level below the

wing decreases (fig. 9(a)), which means that the interaction noise is decreasing. If the jet did not impinge upon the wing-flap system, the sound level would approach a minimum value that includes the noise produced by the nozzle alone plus the reflection of the nozzle noise.

The SPL 1/3-octave spectra for the eight-lobe orifice and the wing with the various flap settings are shown in figure 9(b). The SPL for the deflected flaps ( $10^{\circ}$ - $20^{\circ}$ ,  $30^{\circ}$ - $60^{\circ}$ ) is greater than the SPL for the retracted flaps in the frequency range from 1250 to 6300 hertz. There is a sizeable drop in the SPL in the region around 1000 hertz for the retracted case.

Moving the orifice an additional 1.27 centimeters away from the wing ( $30^{\circ}$ - $60^{\circ}$  flap setting), in order to reduce the scrubbing action, gave results the same as those shown in figure 9 for the normal orifice location.

The noise data for the eight-lobe orifice used with the  $30^{\circ}$ - $60^{\circ}$  flaps, at various orifice pressure ratios (or exhaust velocities), are shown in figure 10. The OASPL (fig. 10(a)) decreases with decreasing pressure ratio but maintains similar directivity patterns. The SPL 1/3-octave spectra (fig. 10(b)) peak at 2500 hertz for all pressure ratios tested.

The noise data for the eight-lobe orifice and the single orifice, both used with the  $30^{\circ}$ - $60^{\circ}$  flaps, are compared in figure 11. Also included are the data for the orifices alone. The OASPL (fig. 11(a)) with the single orifice with the flaps is higher than with the eight-lobe orifice for all angles from the engine inlet. The SPL 1/3-octave spectra below the wing (fig. 11(b)) show a peak at 2500 hertz for both configurations. The spectrum for the single orifice has a higher level in the high-frequency range than the eight-lobe orifice when both are used with the  $30^{\circ}$ - $60^{\circ}$  flaps.

The noise data for the eight-lobe orifice and for a 5.08-centimeter-diameter single nozzle scaled up to the eight-lobe orifice size, both used with the  $10^{\circ}$ - $20^{\circ}$  flaps, are compared in figure 12. Also shown in the figure are data for the orifice and nozzle alone. The data for the single nozzle are from reference 2, and the method of scaling is given in reference 3. The OASPL (fig. 12(a)) shows that the single nozzle is approximately 2 decibels louder under the wing than the eight-lobe orifice when both are used with the  $10^{\circ}$ - $20^{\circ}$  flaps. The SPL spectrum for the single nozzle used with the flaps (fig. 12(b)) peaks at 1600 hertz, whereas the spectrum for the eight-lobe orifice used with the flaps is relatively flat over a large portion of the frequency range.

Sideline noise tests. - Results of the sideline noise tests with the eight-lobe orifice and the  $30^{\circ}$ - $60^{\circ}$  flaps are shown in figure 13. For these tests the wing was placed in a horizontal position so that the fixed portion of the wing was parallel to the plane of the microphone circle and the extended flaps were pointing upward. The OASPL with the wing horizontal is compared to the OASPL with the wing vertical in figure 13(a). The sideline OASPL directivity (with the wing horizontal) is nearly symmetrical about the

orifice axis and is about 6 decibels less than the level under the wing at  $80^{\circ}$ . The SPL 1/3-octave spectra (fig. 13(b)) show that the sideline noise has a lower level high-frequency content.

The sideline noise data for the eight-lobe orifice and zero (retracted) flaps are shown in figure 14. The OASPL with the wing horizontal is compared to the OASPL with the wing vertical in figure 14(a). Again, the OASPL with the wing horizontal is, in general, lower than that with the wing vertical. The SPL 1/3-octave spectra at  $80^{\circ}$  from the engine inlet (fig. 14(b)) show that the sideline noise does not exhibit the minimum level at 1000 hertz that is shown by the spectrum for the vertically oriented wing-flap system.

Variations to orifice-wing system. - A series of experiments were performed employing several variations to the eight-lobe orifice-wing combination. The objective of this series of tests was to try to reduce the noise generated by the presence of the flap slots. For this series of tests the flaps were placed in the  $10^{\circ}$ - $20^{\circ}$  and retracted settings. The orifice pressure ratio was 1.74.

The first variation consisted of blocking off the slots between the fixed wing and the leading flap and between the leading flap and trailing flap. Two separate shields were used: a full shield that covered the entire underside of the wing-flap system, and a partial shield 12.7 centimeters wide centered about the jet axis.

The results of the tests with the eight-lobe orifice blowing on the  $10^{\circ}$ - $20^{\circ}$  flaps when these shield systems were used are shown in figure 15. The data for the  $10^{\circ}$ - $20^{\circ}$  flaps with no shield and the data for the orifice alone are also shown for comparison. The OASPL (fig. 15(a)) for the wing with the shields is slightly lower than that for the wing with no shield. No difference in level exists in the OASPL for full and partial shield systems. A plot of the SPL spectra at  $80^{\circ}$  (fig. 15(b)) shows that the spectra for the wing with the shields has a minimum level at 1600 hertz. The shape of the spectrum for the eight-lobe orifice and  $10^{\circ}$ - $20^{\circ}$  flaps with the shield is similar to that obtained with the eight-lobe orifice and retracted flaps (fig. 9(b)).

Figure 16 shows the results obtained, when the slots were alternately covered, with the wing flaps in the  $10^{\circ}$ - $20^{\circ}$  setting. For this test a thin metal plate was used to completely cover the front slot with the rear slot open and then to cover the rear slot with the front slot open. Also shown in figure 16 are the data obtained when both slots were open and also when both slots were covered (full shield). The OASPL (fig. 16(a)) shows very little difference in levels between  $0^{\circ}$  and  $140^{\circ}$  from the engine inlet for these configurations. The SPL spectra at  $80^{\circ}$  (fig. 16(b)) show that in the region around 1600 hertz a greater reduction in sound level occurs when the rear slot is covered than when the front slot is covered.

These tests with the slots shielded were all performed at the relatively high orifice pressure ratio (1.74), or exhaust velocity. Data obtained in a more extensive experimental program (ref. 2) indicate that the effect of slots on the noise generation becomes

more pronounced at low exhaust velocities. Hence, shielding could have more of an effect at lower velocities.

Another variation consisted of modifying the eight-lobe orifice by mounting a fine-mesh wire screen over the three openings nearest the underside of the wing. The effect of the screen is to induce a lower jet velocity downstream of the orifice. Velocity profiles for the orifice alone for this configuration are shown in figure 17. The wing would be located toward the ordinate side of the figure. At a distance of 15.2 centimeters downstream of the orifice (fig. 17(a)) the velocity from the screened lobes is nearly one-half that from the open lobes. As the distance downstream increases the flow coalesces into a single jet.

Sound data were taken with the modified eight-lobe orifice blowing on the  $10^{\circ}$ - $20^{\circ}$  flaps with and without a full shield blocking the flap slots. Figure 18(a) shows little difference in the OASPL between the wing with and without the shield. Figure 18(b) also shows little difference in the SPL spectra between the two arrangements. The separation in sound pressure level in the frequency range around 1600 hertz is slight compared to similar tests with the unmodified eight-lobe orifice (fig. 16(b)).

The effectiveness of the modified eight-lobe orifice compared to that of the eight-lobe orifice with all lobes open is shown in figure 19. The difference in OASPL between the orifices with the  $10^{\circ}$ - $20^{\circ}$  flaps (without shields) and the orifices alone is plotted as a function of the angle from the engine inlet. A 1- to 2-decibel reduction in sound pressure level is obtained with the modified orifice and the  $10^{\circ}$ - $20^{\circ}$  flaps.

A final variation to the externally-blown-flap system with the eight-lobe orifice with all lobes open and the  $0^{\circ}$  (retracted) flap setting consisted of moving the wing an additional 3.81 centimeters away from the orifice so that the jet did not impinge on and/or scrub the wing surface. The OASPL for this arrangement (fig. 20(a)) shows a reduction in level, compared to the level obtained from the normal wing-orifice position, to approximately  $10^{\circ}$  from the engine inlet. The SPL spectra at  $80^{\circ}$  (fig. 20(b)) show a peak at 500 hertz and then a minimum level at 1000 hertz for both wing positions. Above 1000 hertz the noise with the wing moved away from the orifice is the reflection of the orifice noise with a 3-decibel separation.

## Sound Measurements with 4.1-Centimeter- Equivalent-Diameter Orifices

Orifices alone. - The noise data for the 16-hole orifice alone and a single orifice alone are compared in figure 21. Both orifices had the same total exit area and consequently the same equivalent diameter. In figure 21(a), the sound directivity is shown to be approximately the same for both orifices, with only slight differences in level. The

SPL spectra for the orifices at  $80^{\circ}$  from the engine inlet are shown in figure 21(b). The single orifice has a greater sound level in the middle-frequency range of the spectra whereas in the high-frequency range the 16-hole orifice level is greater. The high-frequency noise content of the 16-hole orifice is characteristic of multielement orifices.

Orifices with wing. - The noise data for the single and 16-hole orifices with the wing in place and the flaps at the  $30^{\circ}$ - $60^{\circ}$  setting are compared in figure 22. The results are similar to those found for the 6.0-centimeter-equivalent-diameter orifices. The OASPL (fig. 22(a)) for the single orifice is greater than that for the 16-hole orifice. This is a result of the lower impingement velocity obtained with the multihole orifice. The spectra for these two conditions (fig. 22(b)) show that the single-orifice configuration has a much higher sound level from a frequency of 1000 to 5000 hertz, with a peak at 2500 hertz. The spectrum with the 16-hole orifice is relatively flat over a large portion of the frequency range.

## SUMMARY OF RESULTS

The results of noise tests of simulated mixer-type nozzles (orifices) used with a model of an externally-blown-flap lift-augmentation system can be summarized as follows:

1. With the  $30^{\circ}$ - $60^{\circ}$  flap setting, the overall sound pressure level (OASPL) under the wing was 4 to 6 decibels less with the multielement orifices than with a single orifice. With the  $10^{\circ}$ - $20^{\circ}$  flap setting, the OASPL under the wing was approximately 2 decibels less with the multielement orifice.

2. Sideline noise level, with the  $30^{\circ}$ - $60^{\circ}$  flap setting, was 6 decibels less than the noise level under the wing ( $80^{\circ}$  to  $100^{\circ}$  from engine inlet). With the zero flap setting, the sideline noise level was 4.5 decibels less than the noise level under the wing.

The results of noise tests for variations to the eight-lobe orifice - wing - flap system can be summarized as follows:

1. Shielding both leading edges of the flaps from the jet, with the  $10^{\circ}$ - $20^{\circ}$  flap setting, reduced the OASPL under the wing by approximately 2 decibels.

2. Covering the rear slot, with the  $10^{\circ}$ - $20^{\circ}$  flap setting, had a greater effect on the sound pressure level (SPL) spectra at  $80^{\circ}$  than covering the front slot.

3. Reducing the velocity next to the wing reduced the interaction noise by approximately 1.5 to 2 decibels.

4. With the  $0^\circ$  flap setting, increasing the distance from the wing to the orifice, so that no impingement occurred on the wing surface, reduced the OASPL by 2 to 4 decibels ( $0^\circ$  to  $120^\circ$  from the engine inlet).

Lewis Research Center,  
National Aeronautics and Space Administration,  
Cleveland, Ohio, June 29, 1972,  
741-89.

## REFERENCES

1. Groesbeck, D.; Huff, R.; and von Glahn, U.: Peak Axial-Velocity Decay with Mixer-Type Exhaust Nozzles. NASA TM X-67934, 1971.
2. Olsen, William A.; Dorsch, Robert G.; and Miles, Jeffrey H.: Noise Produced by a Small-Scale, Externally Blown Flap. NASA TN D-6636, 1972.
3. Dorsch, R. G.; Kreim, W. J.; and Olsen, W. A.: Externally-Blown-Flap Noise. Paper 72-129, AIAA, Jan. 1972.

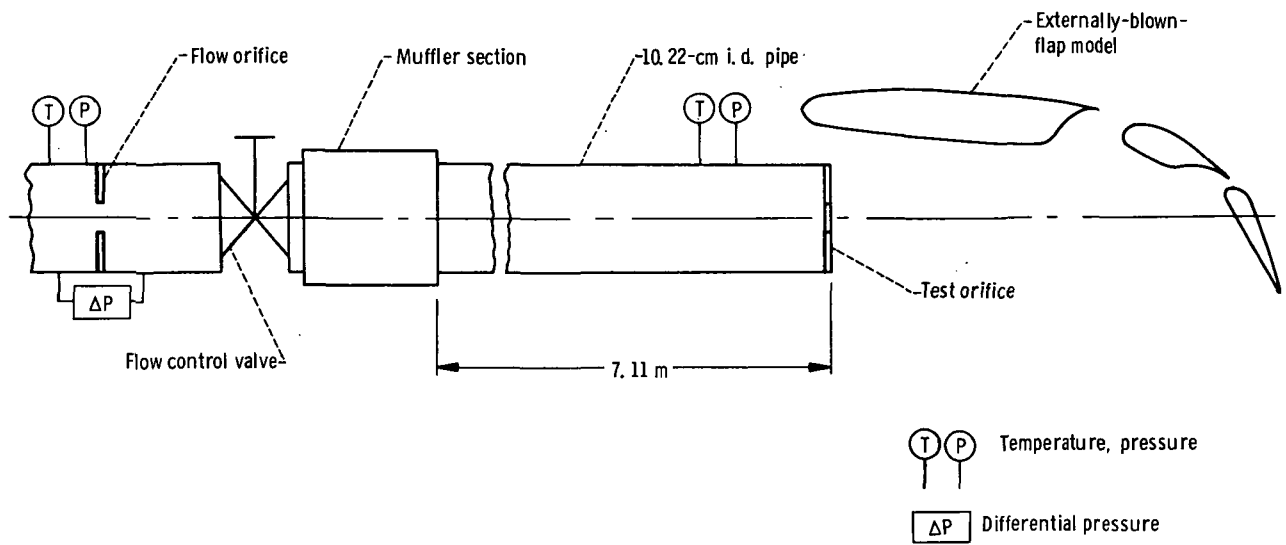
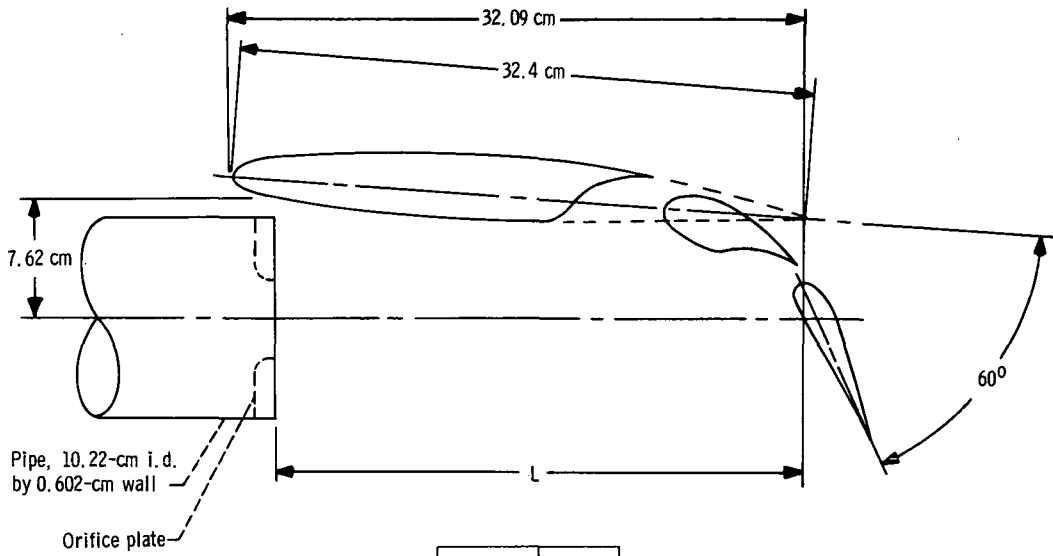
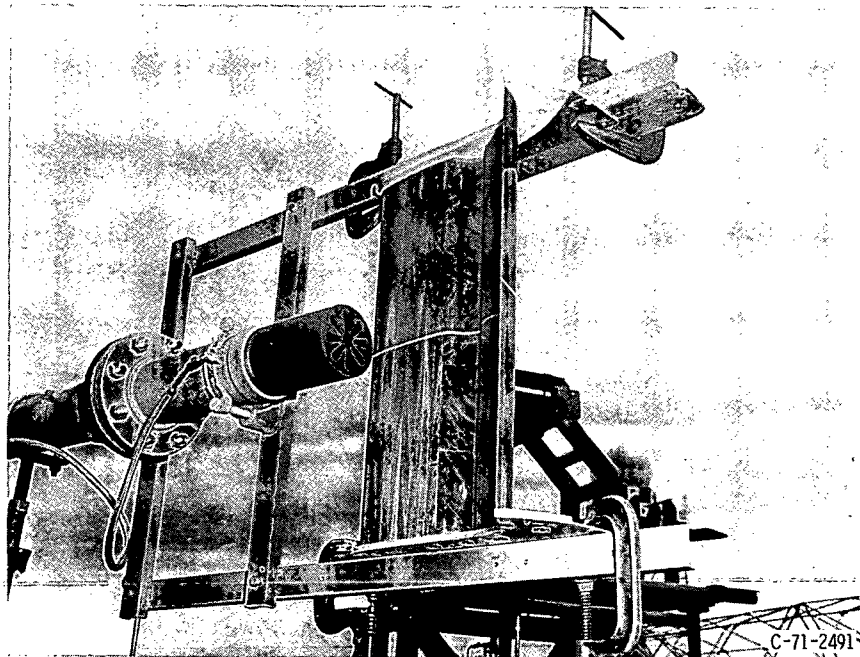


Figure 1. - Flow system.



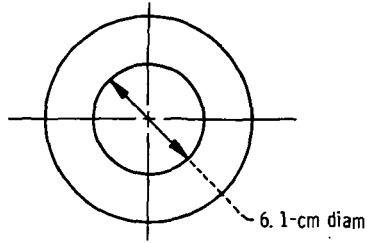
Orifice equivalent diameter, cm	Length, L, cm
6.0	29.55
4.1	37.0

(a) Wing-flap assembly. Wing span, 61 cm.

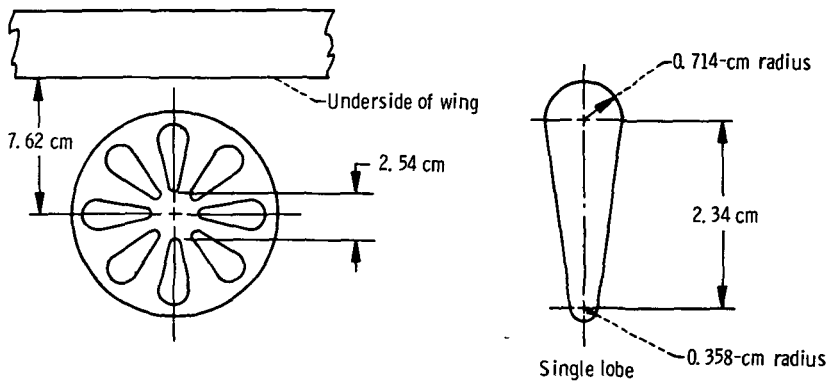


(b) Externally blown flap with eight-lobe orifice plate.

Figure 2. - Test configuration.

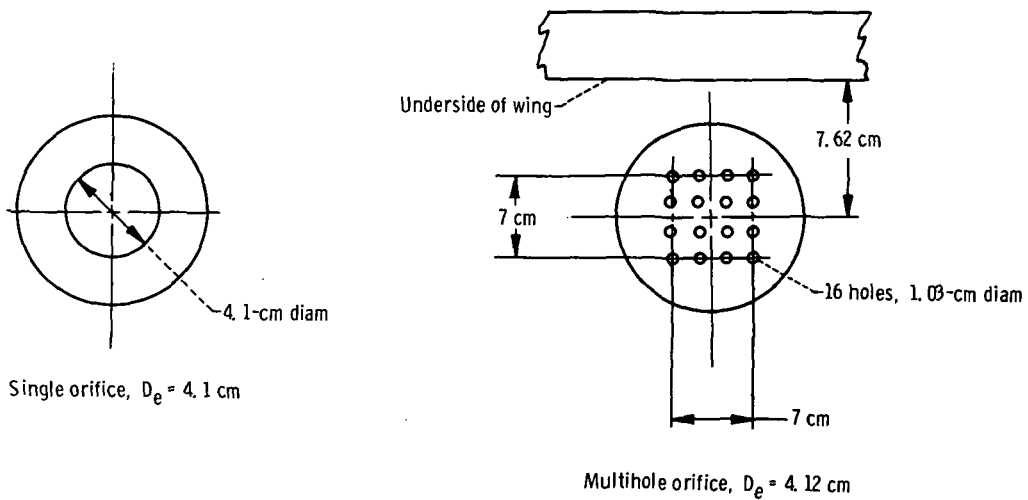


Single orifice,  $D_e = 6.1$  cm



Eight-lobe orifice,  $D_e = 5.94$  cm

(c) Orifice configurations having 6.0-centimeter (nominal) equivalent diameters  $D_e$ .



Single orifice,  $D_e = 4.1$  cm

Multihole orifice,  $D_e = 4.12$  cm

(d) Orifice configurations having 4.1-centimeter (nominal) equivalent diameters  $D_e$ .

Figure 2. - Concluded.

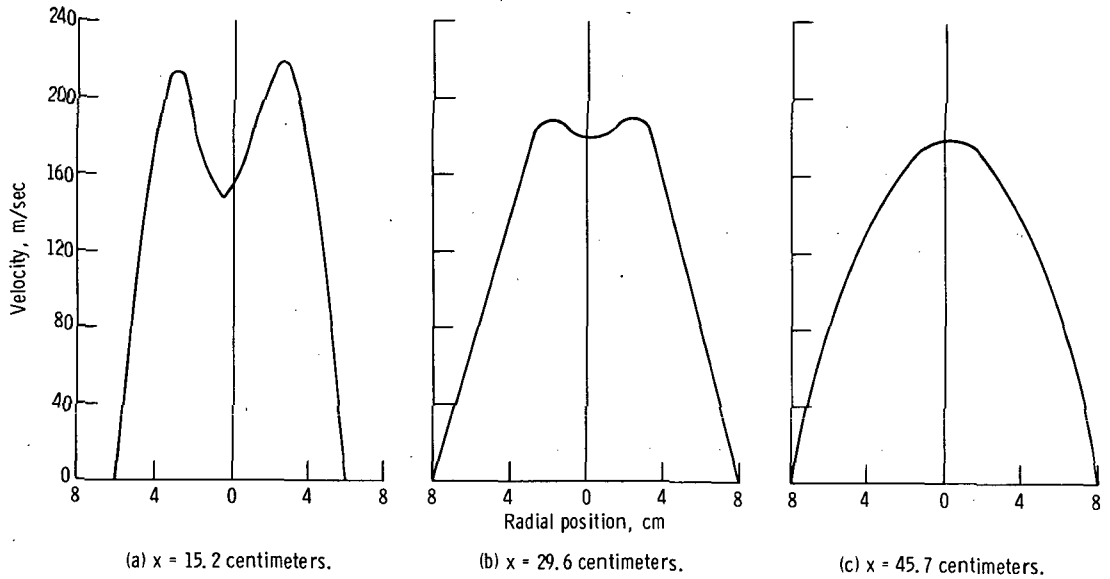


Figure 3. - Velocity profiles at various axial positions  $x$  for eight-lobe orifice. Orifice pressure ratio, 1.7; orifice exhaust velocity, 290 meters per second.

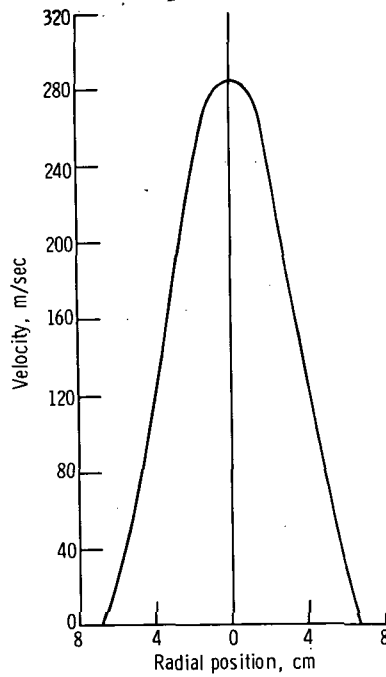


Figure 4. - Velocity profile at axial distance of 29.6 centimeters downstream of the orifice for single 6.1-centimeter-diameter orifice. Orifice pressure ratio, 1.7; orifice exhaust velocity, 290 meters per second.

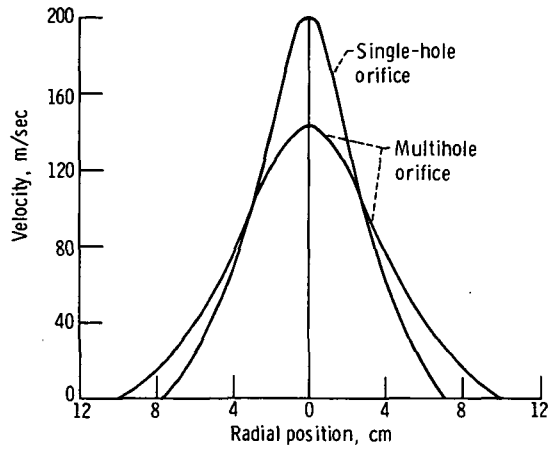


Figure 5. - Velocity profiles at axial distance of 37 centimeters downstream of the orifice for 4.1-centimeter-equivalent-diameter orifices. Orifice pressure ratio, 1.7; orifice exhaust velocity, 289 meters per second.

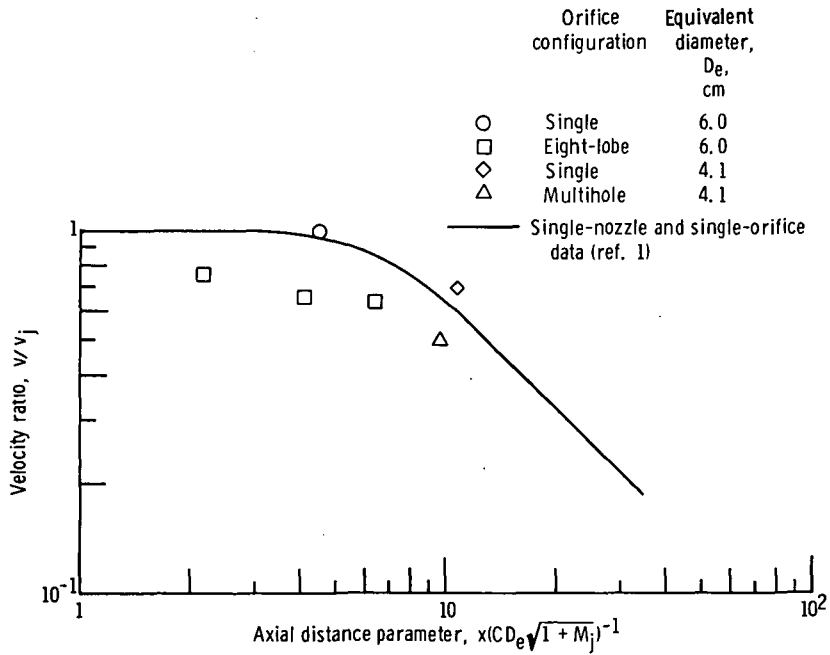
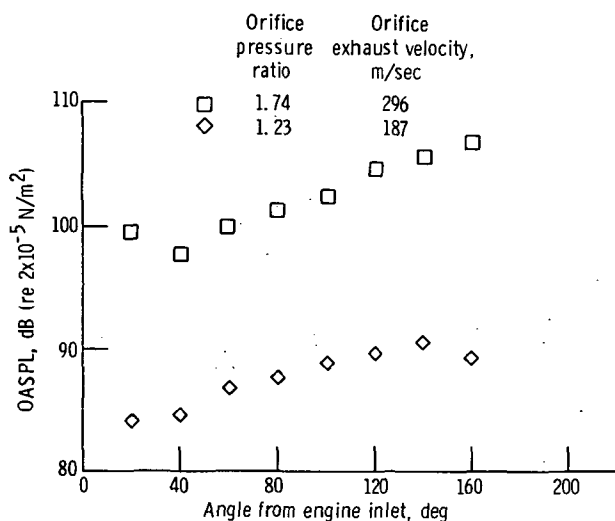
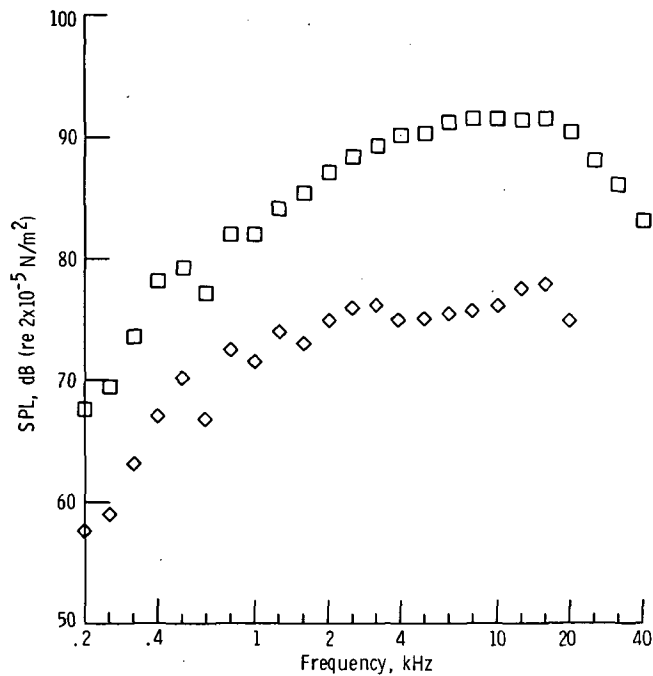


Figure 6. - Comparison of peak axial velocity decay obtained with single and multielement orifices.

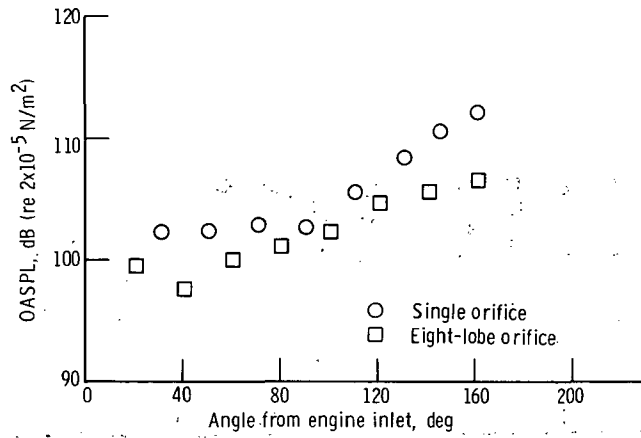


(a) Overall sound pressure level directivity.

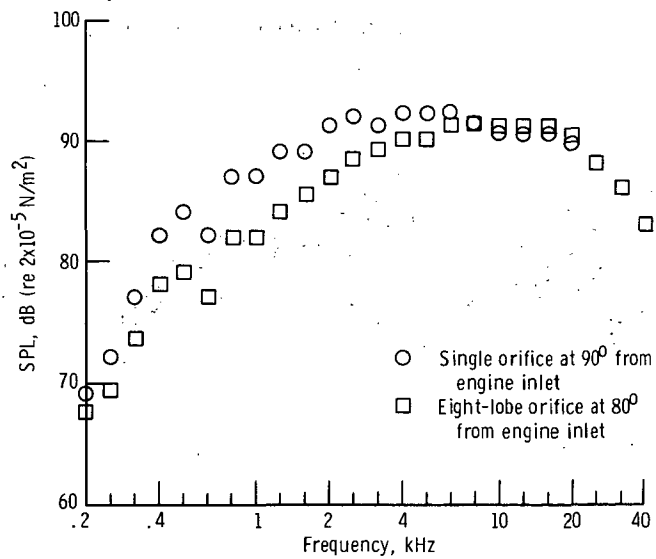


(b) Sound pressure level 1/3-octave spectra at 80° from engine inlet.

Figure 7. - Comparison of noise data for eight-lobe orifice alone at two orifice pressure ratios. Microphone radius, 3.05 meters.

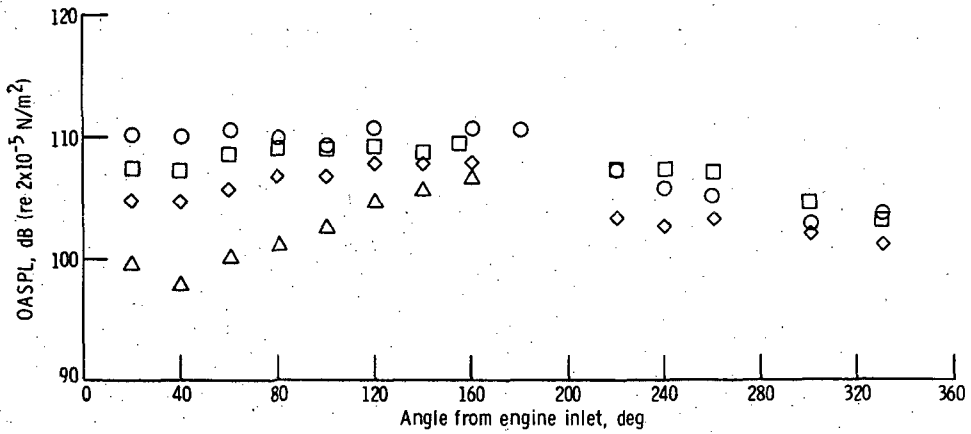


(a) Overall sound pressure level directivity.

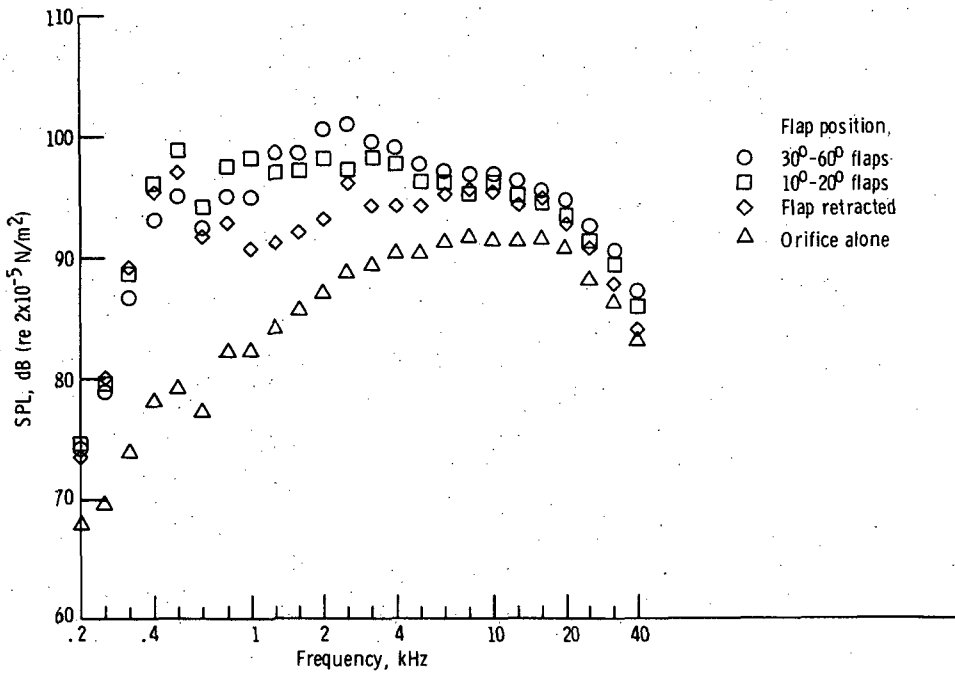


(b) Sound pressure level 1/3-octave spectra.

Figure 8. - Comparison of noise data for single orifice alone and eight-lobe orifice alone. Equivalent diameter, 6.0 centimeters; orifice pressure ratio, 1.74; orifice exhaust velocity, 296 meters per second; microphone radius, 3.05 meters.

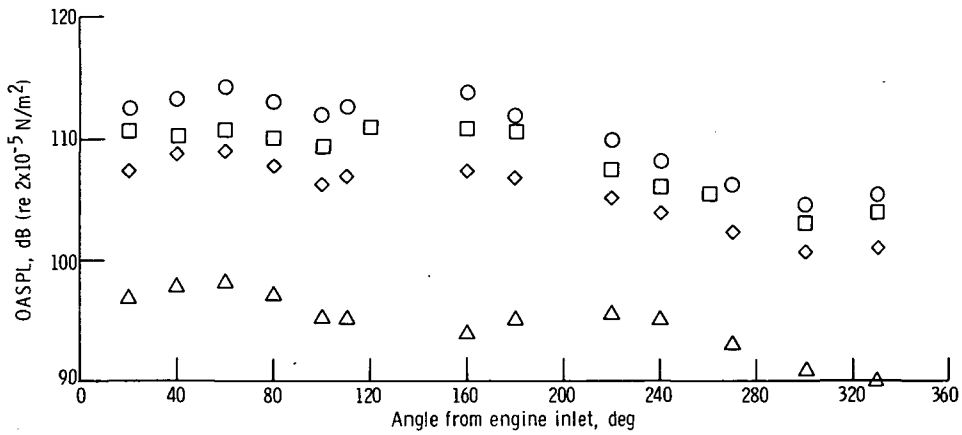


(a) Overall sound pressure level directivity.

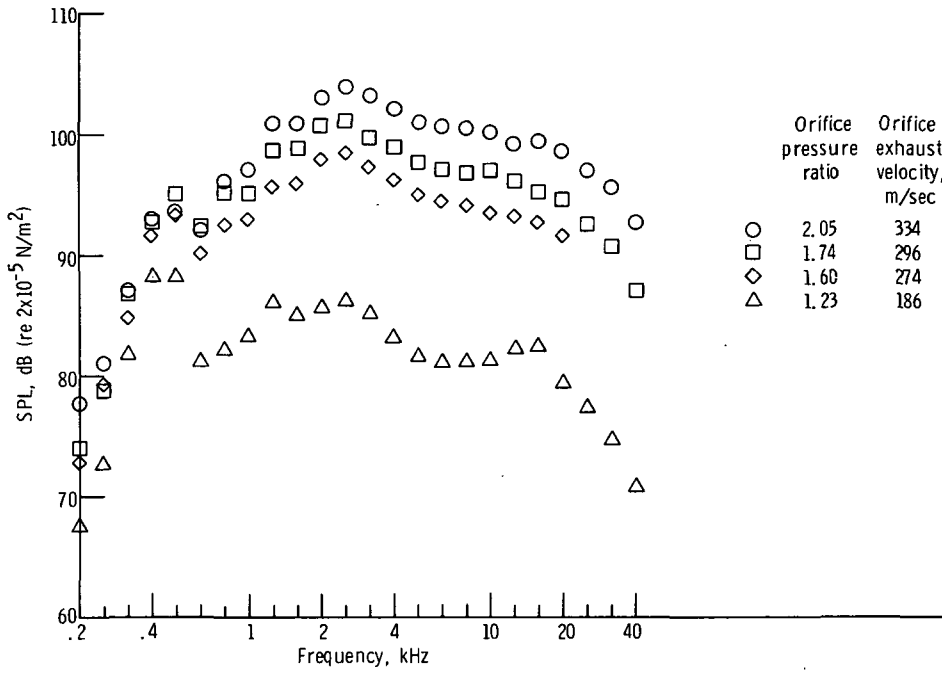


(b) Sound pressure level 1/3-octave spectra at 80° from engine inlet.

Figure 9. Comparison of noise data for various flap positions with the eight-lobe orifice. Orifice pressure ratio, 1.74; orifice exhaust velocity, 296 meters per second; microphone radius, 3.05 meters.

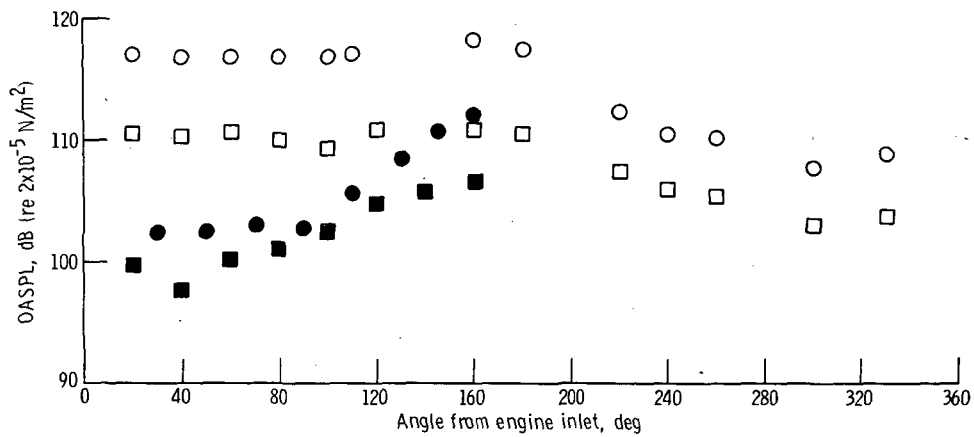


(a) Overall sound pressure level directivity.

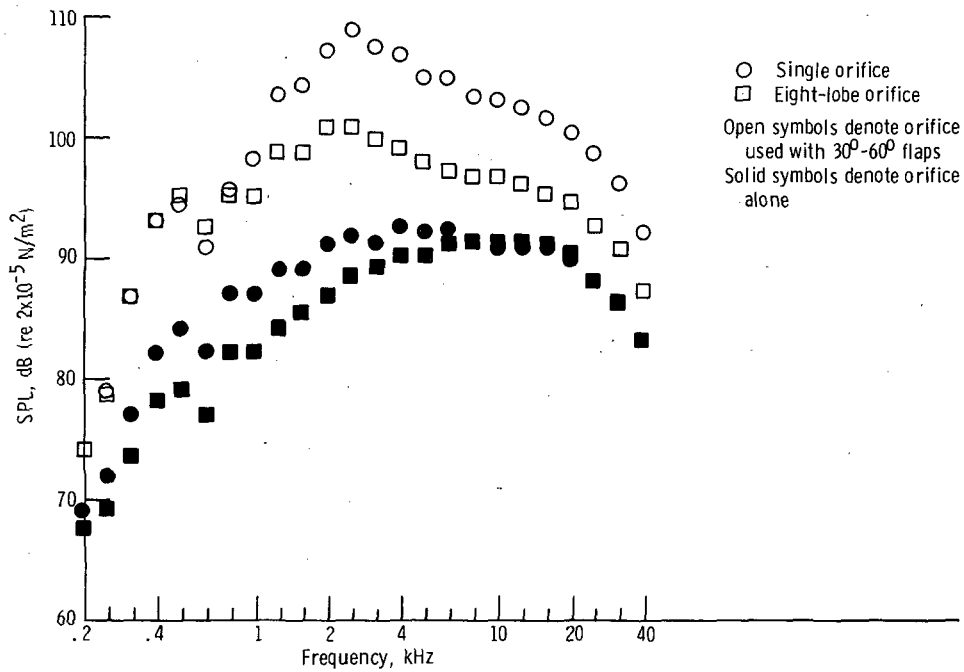


(b) Sound pressure level 1/3-octave spectra at  $80^\circ$  from engine inlet.

Figure 10. - Comparison of noise data at various orifice pressure ratios for eight-lobe orifice and  $30^\circ$ - $60^\circ$  flaps. Microphone radius, 3.05 meters.

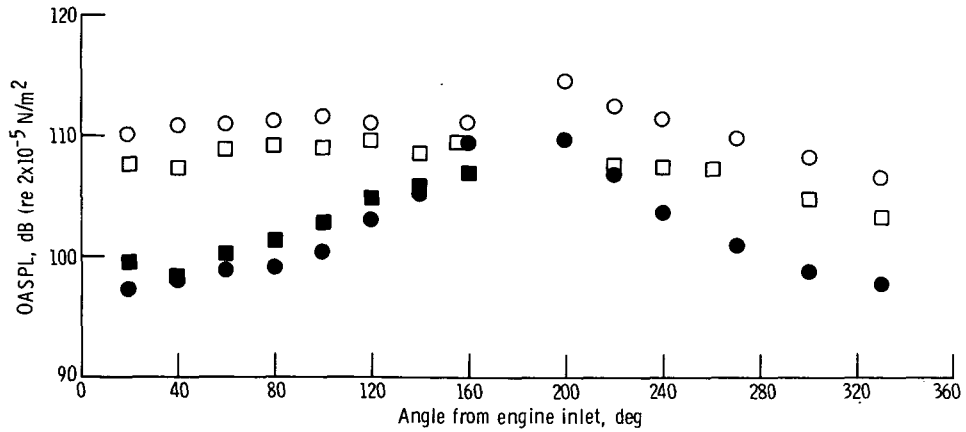


(a) Overall sound pressure level directivity.

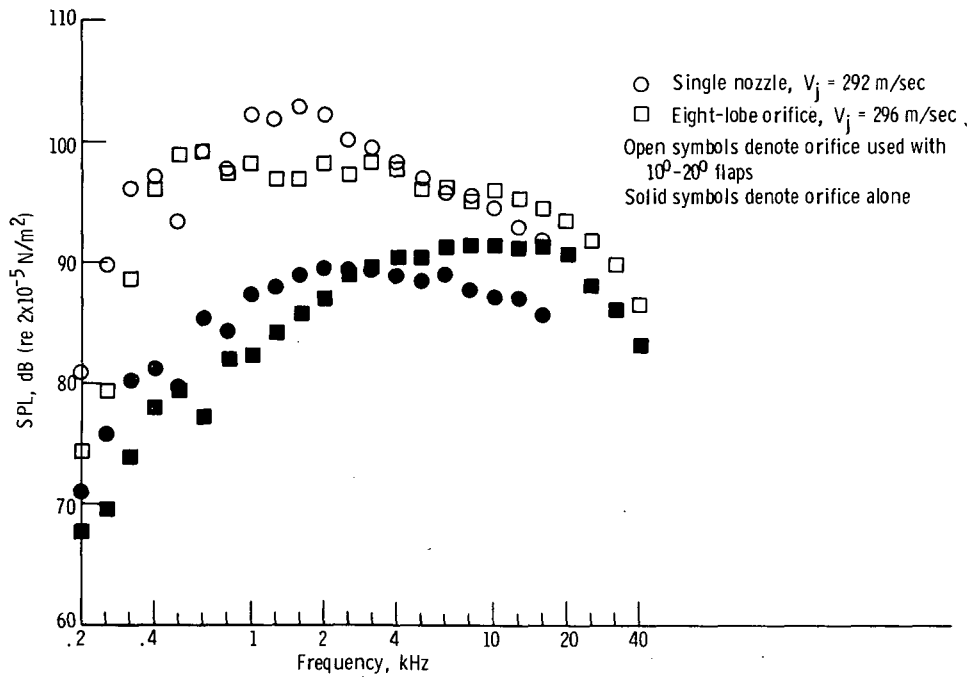


(b) Sound pressure level 1/3-octave spectra below wing at  $80^\circ$  from engine inlet, except for single nozzle alone, which was tested at  $90^\circ$ .

Figure 11. - Comparison of noise data for single and eight-lobe orifices - both alone and with  $30^\circ$ - $60^\circ$  flaps. Orifice pressure ratio, 1.74; orifice exhaust velocity, 296 meters per second; microphone radius, 3.05 meters.

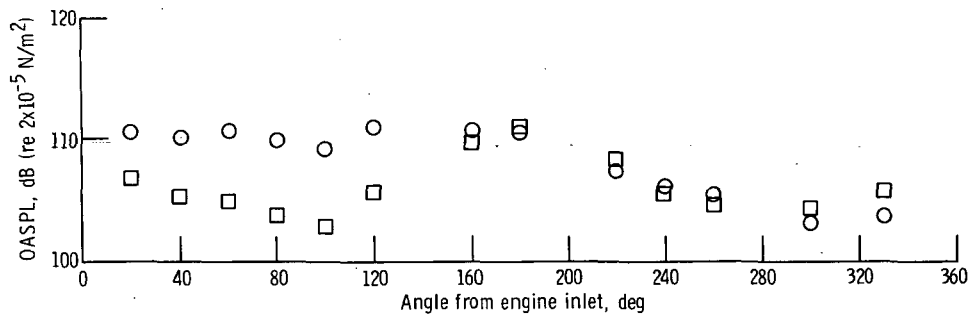


(a) Overall sound pressure level directivity.

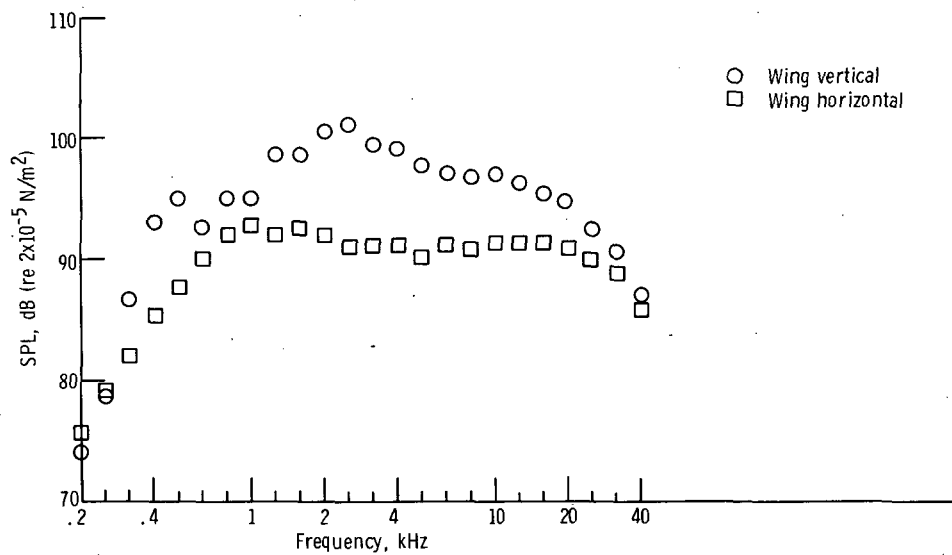


(b) Sound pressure level 1/3-octave spectra at  $80^\circ$  from engine inlet.

Figure 12. - Comparison of noise data for eight-lobe orifice and 5.08-centimeter-diameter single nozzle scaled up to eight-lobe orifice - both alone and used with  $10^0$ - $20^0$  flaps. Orifice pressure ratio, 1.7 (nominal); microphone radius, 3.05 meters.

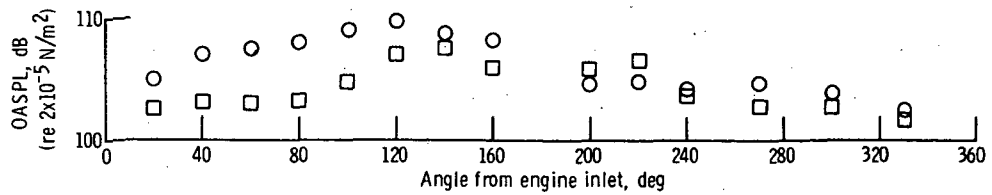


(a) Overall sound pressure level directivity.

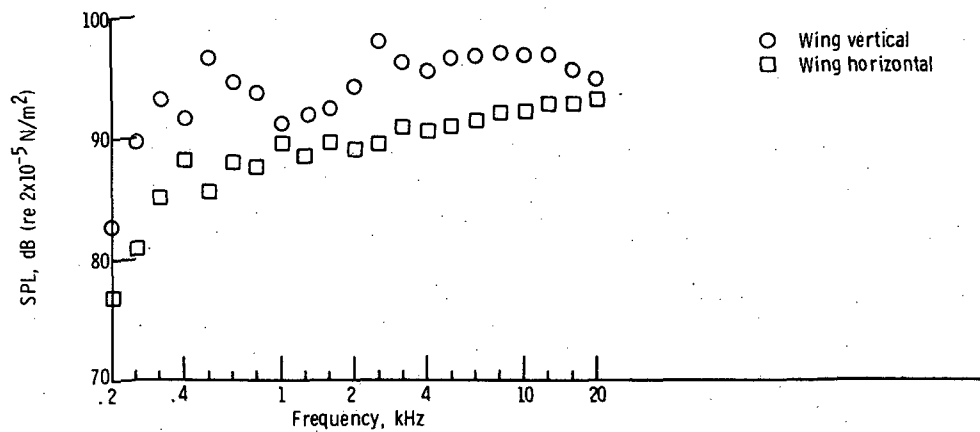


(b) Sound pressure level 1/3-octave spectra at 80° from engine inlet.

Figure 13. - Comparison of noise data for vertical and horizontal (underside of wing facing up) wing positions - eight-lobe orifice with 30°-60° flaps. Orifice pressure ratio, 1.74; orifice exhaust velocity, 296 meters per second; microphone radius, 3.05 meters.

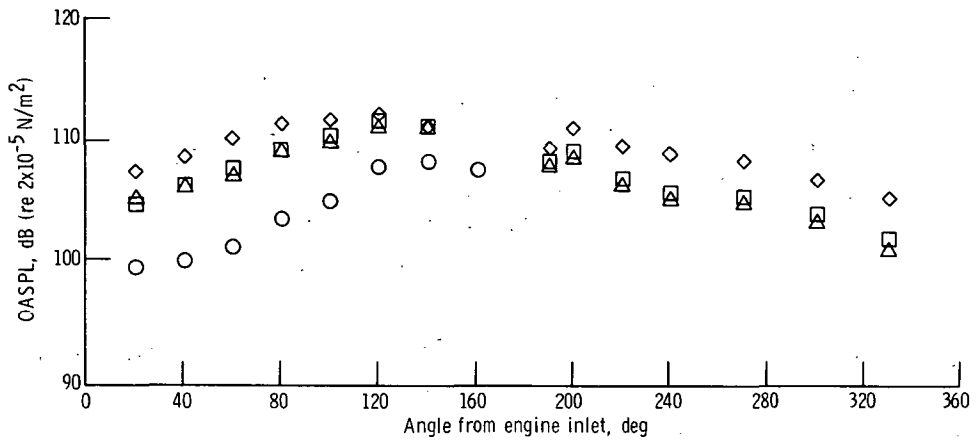


(a) Overall sound pressure level directivity.

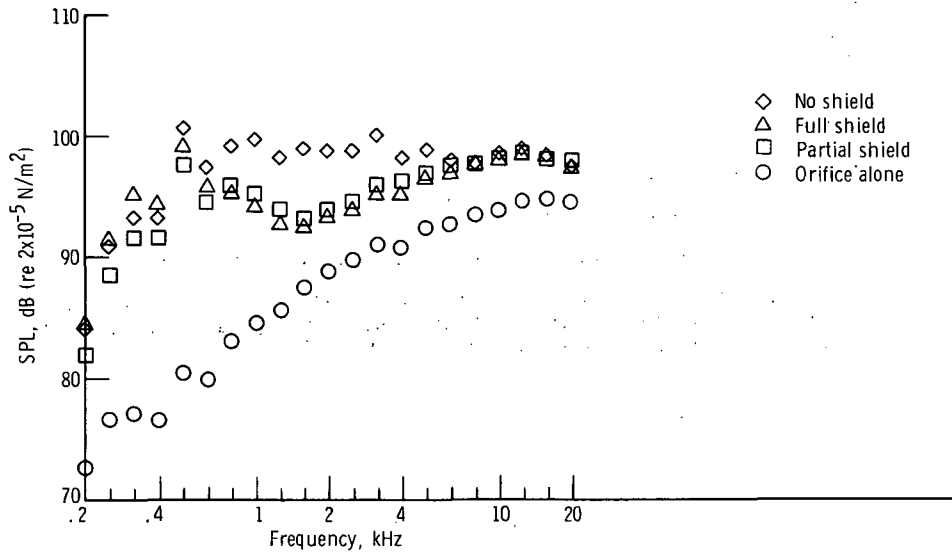


(b) Sound pressure level 1/3-octave spectra at 80° from engine inlet.

Figure 14. - Comparison of noise data for vertical and horizontal (underside of wing facing upward) wing positions - eight-lobe orifice with  $\theta^0$  (retracted) flaps. Orifice pressure ratio, 1.74; orifice exhaust velocity, 296 meters per second; microphone radius, 3.05 meters.

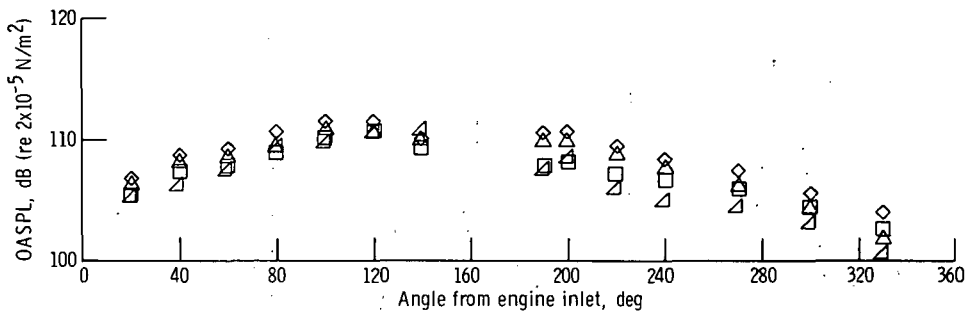


(a) Overall sound pressure level directivity.

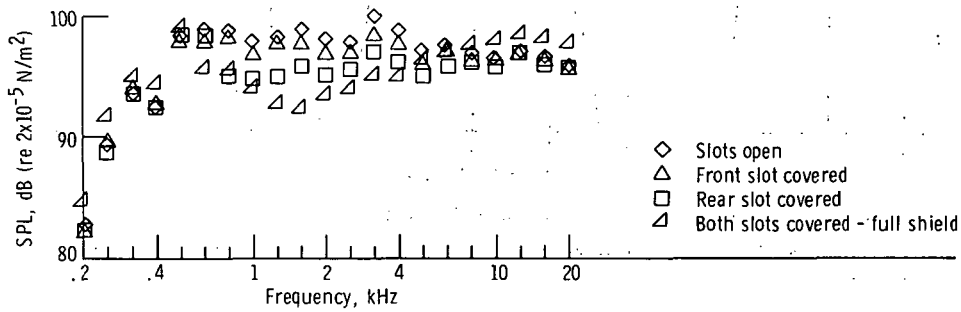


(b) Sound pressure level 1/3-octave spectra at 80° from engine inlet.

Figure 15. - Comparison of noise data for eight-lobe orifice used with 10°-20° flaps with and without shields. Orifice pressure ratio, 1.74; orifice exhaust velocity, 296 meters per second; microphone radius, 3.05 meters.



(a) Overall sound pressure level directivity.



(b) Sound pressure level 1/3-octave spectra at 80° from engine inlet.

Figure 16. - Comparison of noise data for eight-lobe orifice used with 10°-20° flaps with alternate covering of slots. Orifice pressure ratio, 1.74; orifice exhaust velocity, 296 meters per second; microphone radius, 3.05 meters.

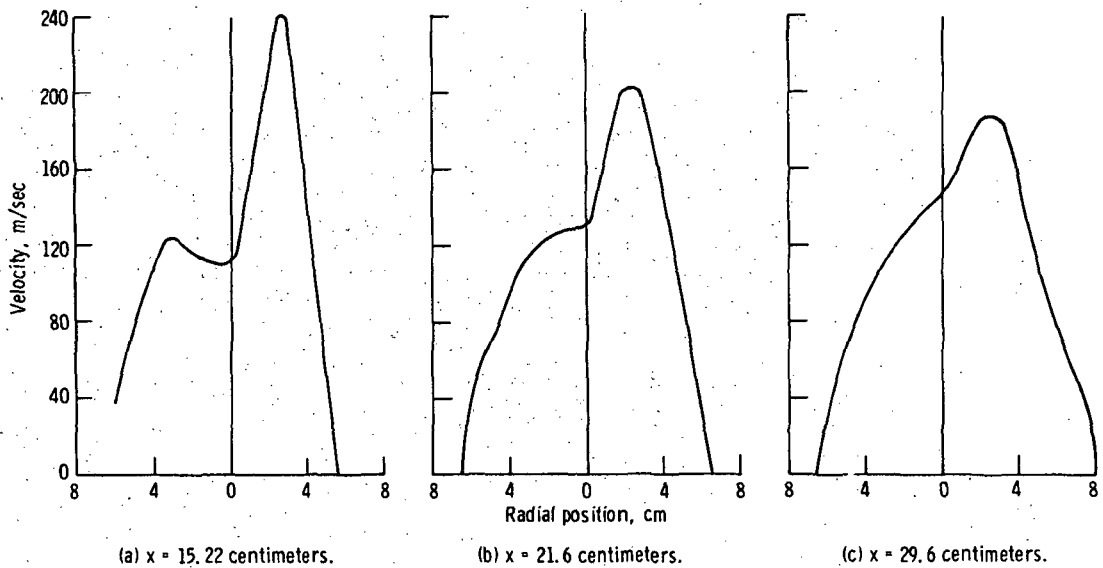
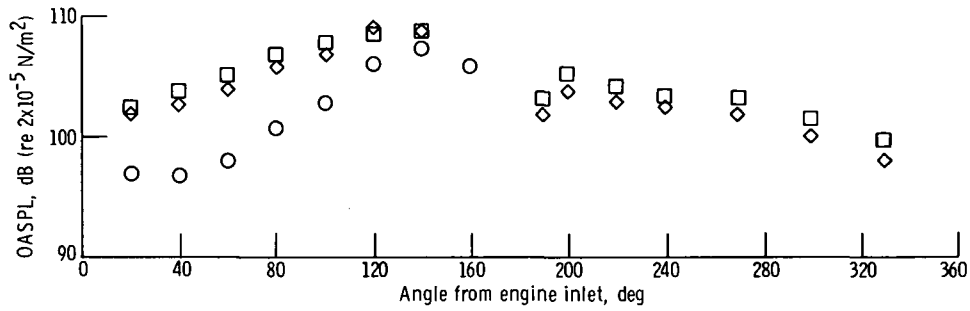
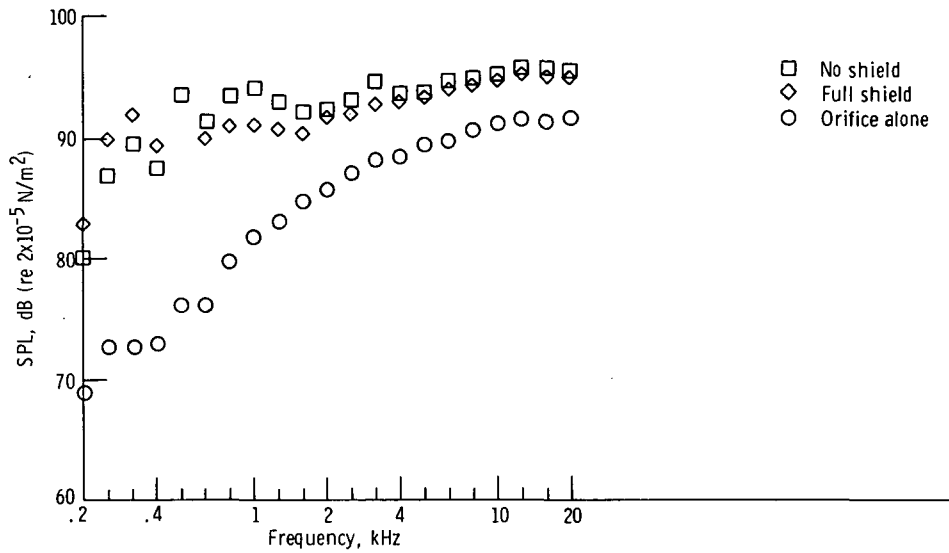


Figure 17. - Velocity profiles at various axial positions  $x$  for eight-lobe orifice with screen over three lobes. Orifice pressure ratio, 1.71.



(a) Overall sound pressure level directivity.



(b) Sound pressure level 1/3-octave spectra at 80° from engine inlet.

Figure 18. - Comparison of noise data for modified eight-lobe orifice (five lobes open and three lobes screened) used with 10°-20° flaps with and without a full shield. Orifice pressure ratio, 1.71; microphone radius, 3.05 meters.

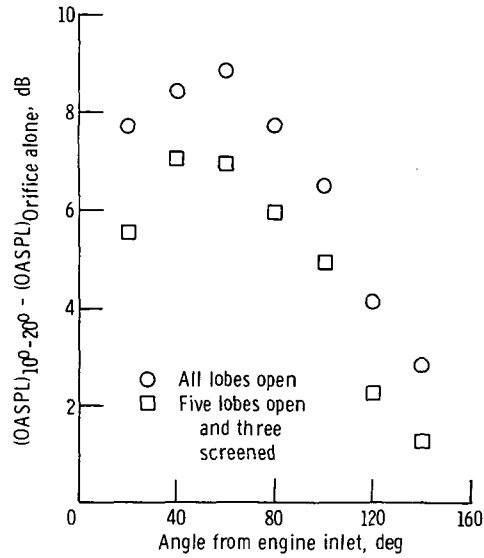
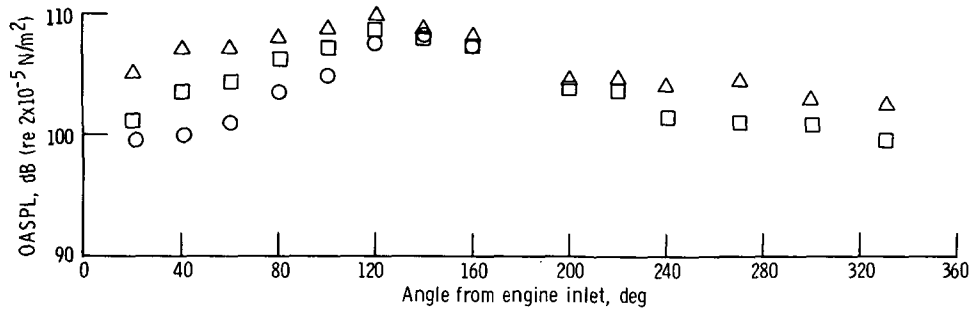
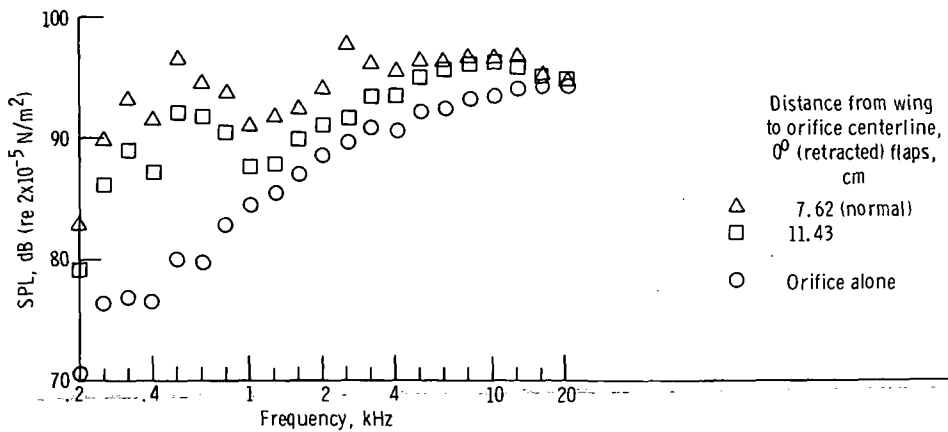


Figure 19. - Difference in sound level when eight-lobe orifice and modified eight-lobe orifice are used with  $10^{\circ}$ - $20^{\circ}$  flaps and used alone. Orifice pressure ratio, 1.7 (nominal); microphone radius, 3.05 meters.

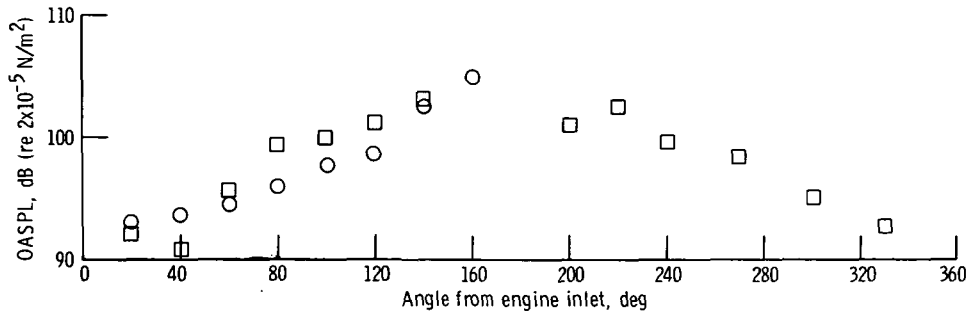


(a) Overall sound pressure level directivity.

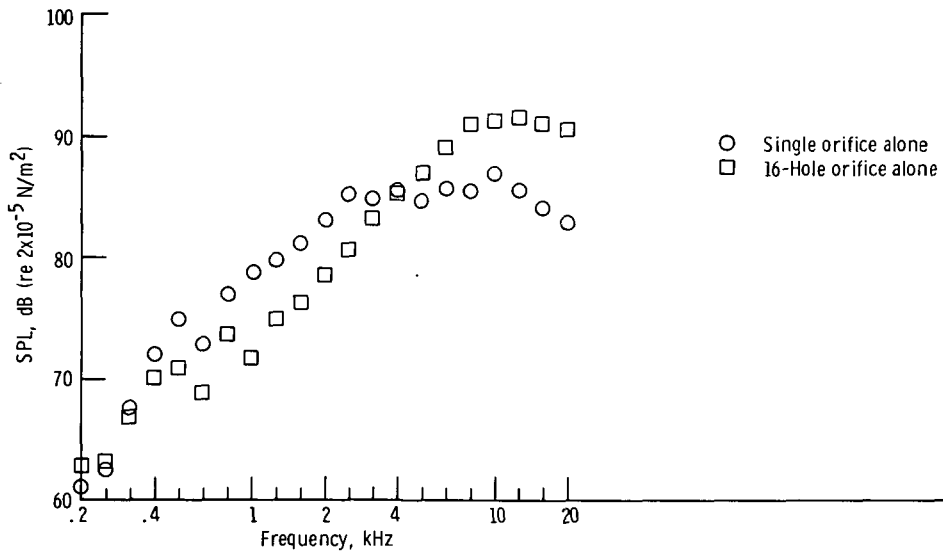


(b) Sound pressure level 1/3-octave spectra at  $80^{\circ}$  from engine inlet

Figure 20. - Comparison of noise data with wing-to-orifice distance varied - eight-lobe orifice with  $0^{\circ}$  (retracted) flaps. Orifice pressure ratio, 1.74; orifice exhaust velocity, 296 meters per second; microphone radius, 3.05 meters.

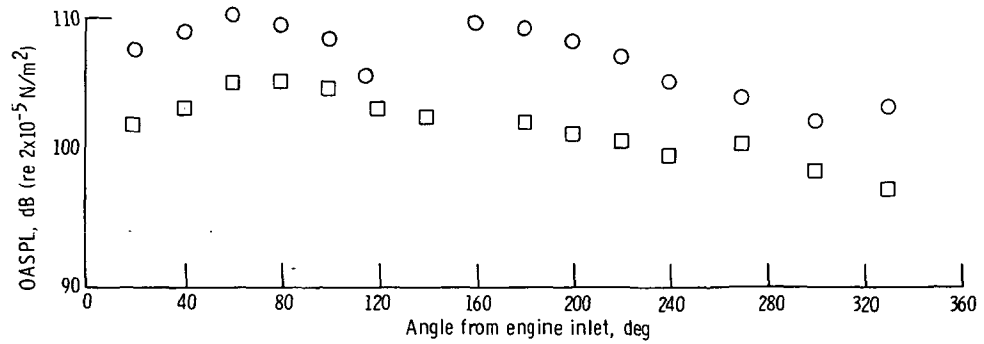


(a) Overall sound pressure level directivity.

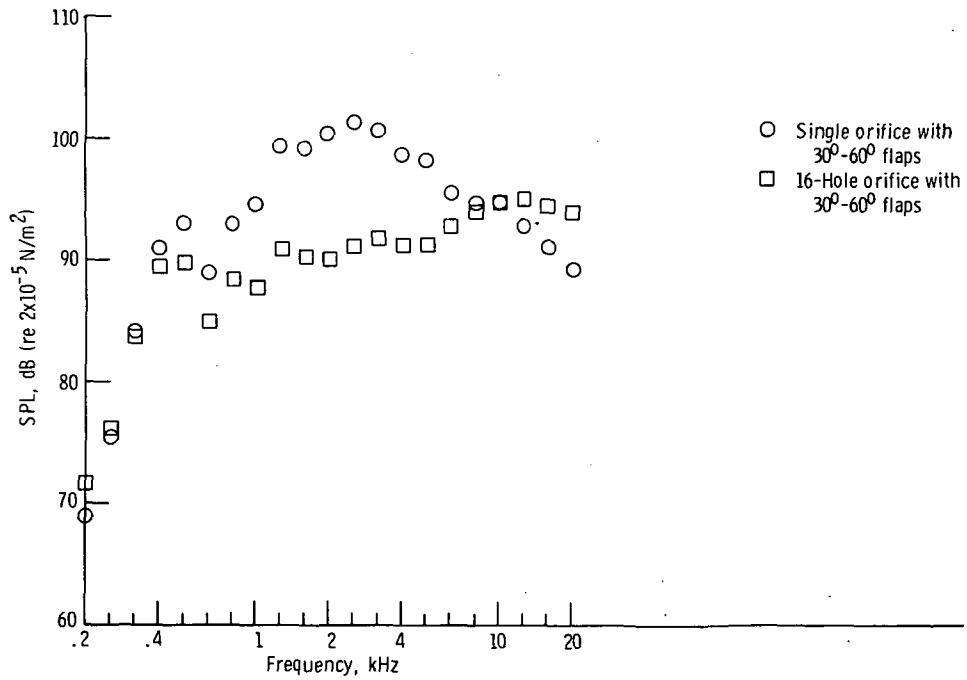


(b) Sound pressure level 1/3-octave spectra at 80° from engine inlet.

Figure 21. - Comparison of noise data for single orifice alone and 16-hole orifice alone. Equivalent diameter, 4.1 centimeters; orifice pressure ratio, 1.7; orifice exhaust velocity, 290 meters per second; microphone radius, 3.05 meters.



(a) Overall sound pressure level directivity.



(b) Sound pressure level 1/3-octave spectra at 80° from engine inlet.

Figure 22. - Comparison of noise data for single and 16-hole orifices used with 30°-60° flaps. Orifice pressure ratio, 1.7; orifice exhaust velocity, 290 meters per second; microphone radius, 3.05 meters.



POSTMASTER:

If Undeliverable (Section 153  
Postal Manual) Do Not Return

*"The aeronautical and space activities of the United States shall be conducted so as to contribute . . . to the expansion of human knowledge of phenomena in the atmosphere and space. The Administration shall provide for the widest practicable and appropriate dissemination of information concerning its activities and the results thereof."*

—NATIONAL AERONAUTICS AND SPACE ACT OF 1958

## NASA SCIENTIFIC AND TECHNICAL PUBLICATIONS

**TECHNICAL REPORTS:** Scientific and technical information considered important, complete, and a lasting contribution to existing knowledge.

**TECHNICAL NOTES:** Information less broad in scope but nevertheless of importance as a contribution to existing knowledge.

**TECHNICAL MEMORANDUMS:** Information receiving limited distribution because of preliminary data, security classification, or other reasons. Also includes conference proceedings with either limited or unlimited distribution.

**CONTRACTOR REPORTS:** Scientific and technical information generated under a NASA contract or grant and considered an important contribution to existing knowledge.

**TECHNICAL TRANSLATIONS:** Information published in a foreign language considered to merit NASA distribution in English.

**SPECIAL PUBLICATIONS:** Information derived from, or of value to NASA activities. Publications include final reports of major projects, monographs, data compilations, handbooks, sourcebooks, and special bibliographies.

**TECHNOLOGY UTILIZATION PUBLICATIONS:** Information on technology used by NASA that may be of particular interest in commercial and other non-aerospace applications. Publications include Tech Briefs, Technology Utilization Reports and Technology Surveys.

Details on the availability of these publications may be obtained from:

SCIENTIFIC AND TECHNICAL INFORMATION OFFICE

NATIONAL AERONAUTICS AND SPACE ADMINISTRATION

Washington, D.C. 20546